Laser cladding of ZrO2-(Ni alloy) composite coating

Pei, Y.T.; Ouyang, J.H.; Lei, T.C.

Published in:
Surface & Coatings Technology

DOI:
10.1016/0257-8972(95)02483-2

Publication date:
1996

ELSEVIER

Surface and Coatings Technology 81 (1996) 131–135

SURFACE & COATINGS TECHNOLOGY

Laser cladding of ZrO_2–(Ni alloy) composite coating

Y.T. Pei, J.H. Ouyang, T.C. Lei

Department of Metals and Technology, Harbin Institute of Technology, Harbin 150001, People's Republic of China

Received 11 March 1994; accepted in final form 15 May 1995

Abstract

The microstructure of laser-clad 60 vol.% ZrO_2 (partially stabilized with 2 mol% Y_2O_3) plus 40 vol.% Ni alloy composite coating on steel 1045 was investigated by scanning electron microscopy, electron probe microanalysis, X-ray diffraction, energy-dispersive X-ray analysis and microhardness tests. The composite coating consists of a pure ZrO_2 clad layer in the outer region and a bonding zone of Ni alloy adjacent to the substrate. The pure ceramic layer exhibits fine equiaxed ZrO_2 grains in the outer zone and columnar ZrO_2 dendrites in the inner zone, growing from the ceramic layer–bonding zone interface. This ceramic layer is composed of metastable t'-ZrO_2 phase and a very small amount of m-ZrO_2 phase and displays a microhardness of 1700 $HV_{0.2}$. The high heating and cooling rate caused by laser cladding restrains the t→m phase transformation in the ZrO_2 ceramic layer. Interdiffusion of alloy elements takes place in the bonding zone, in which the coexistence of ZrO_2 particles, Ni-based solid solution and $(Fe,Cr)_{23}C_6$ particles in the interdendritic regions was found.

Keywords: Microstructure; Composite coatings; Laser cladding

1. Introduction

Zirconia coatings are widely used for thermal protection of high temperature components in gas turbines and diesel engines. Plasma spraying is a common method for producing ceramic coatings on metals or alloys. However, cracking and porosity are major problems associated with plasma-sprayed coatings. The highly porous and crack structure usually makes the ceramic coatings permeable to atmospheric gases and liquids, resulting in the failure of both thermal and chemical barriers.

In recent years, there has been a widespread interest in sealing the porosity in plasma-sprayed ceramic coatings by laser surface melting [1–5]. This method can offer a better microstructure and homogeneity to improve the bond strength and to reduce the porosity by remelting the coating material. Studies [5–9] on laser sealing of plasma-sprayed zirconia coatings reveal the presence of macro- and microcracks after the laser treatment. Therefore, it is interesting to make the zirconia coating directly by using a laser cladding technique.

In the work reported in this paper, an attempt was made on the laser cladding of ZrO_2 ceramic coatings. In order to minimize the thermal expansion coefficient mismatches between ceramic coating and substrate steel, a mixture of 2 mol% yttria–partially stabilized zirconia and Ni–Cr–B–Si alloy powders was used as the coating material. The optimum processing parameters and microstructure of the ceramic coating were carefully analysed.

2. Experimental procedure

Commercial steel 1045 was used as the substrate and a mixture of 60 vol.% ZrO_2 (partially stabilized with 2 mol% Y_2O_3) ceramics plus 40 vol.% Ni alloy powders as coating material. The normal composition of steel 1045 is (weight per cent) 0.45 C, 0.22 Si, 0.52 Mn and Fe in balance. The chemical composition of the Ni alloy powder is (weight per cent) 15.0 Cr, 4.0 B, 5.8 Si, 0.73 C, 12.3 Fe and Ni in balance. The particle size of the Ni alloy powders is about 30 μm and that of the ZrO_2 powders is 0.1–1.0 μm. The thickness of preplaced coating material is about 0.5 mm.

A 2 kW continuous wave CO_2 laser was employed to produce single clad tracks with no overlap under the processing conditions of 800–1000 W laser power, 2–12 mm s^{-1} scanning speed of the laser beam and a 3 mm beam diameter. Argon was blown to shroud the molten pool from the outside atmosphere.

The transverse sections of the clads were cut for

SSDI 0257-8972(95)02483-2

microstructural studies. Electrolytic etching with a 1 mol% NaOH solution was firstly used to attack the bonding zone of Ni alloy; then 4% Nital was chosen to reveal the heat-affected zone of the substrate. The pure ZrO_2 clad layer, stratified from the mixed powder during laser melting, was specially eroded with boiled hydrofluoric acid for 5 s.

Microstructural observations were carried out using a Hitachi S570-type scanning electron microscope and a JCXA-733 electron probe. The phases present in the original powder and laser clad coating were identified using a D/MAX-RB type X-ray diffractometer with Cu Kα radiation. A step scanning mode was used for more detailed phase analysis with a 0.05° step in 2θ over the high 2θ range from 72° to 76° for detecting t′(004, 400) peaks.

3. Results and discussion

3.1. Microstructural analysis

The cross-section of the composite coating typically observed in laser-clad specimens is shown in Fig. 1. It can be seen that the white ceramic layer with a side angle of 138° cannot be easily etched by conventional metallographic techniques (Fig. 1(a)). The HF acid etching reveals that a homogeneous and dense ceramic coating about 0.15 mm thick is obtained with an absence of porosity and microcracks (Fig. 1(b)). This shows that the technological parameters selected in this study ensure a high quality of laser cladding.

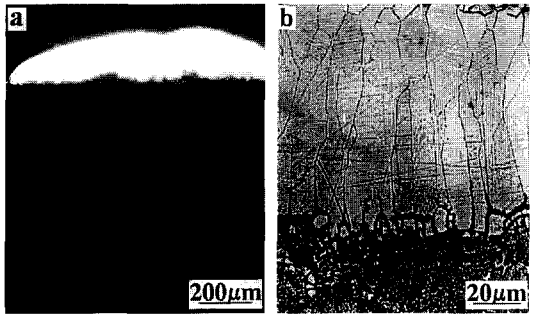

Fig. 1. Cross-section of laser clad ZrO_2–(Ni alloy) composite coating on steel 1045 ($P = 1000$ W, $V = 10$ mm s^{-1} and $D = 3$ mm): (a) etched by 1 mol% NaOH electrolyte; (b) etched by boiled HF acid.

Fig. 2 shows the microstructural characteristics of the bonding zone between the ceramic layer and substrate. There occurs a redistribution of the mixed powders during laser melting. Boosted by the convection in the laser-molten pool, a strong affinity of the Ni alloy melt with the steel substrate and the lower density of ZrO_2 compared with Ni alloy melts led to a segregation of Ni alloy elements at the lower zone and the ZrO_2 ceramics at the upper zone of the molten pool. As a result, a layering phenomenon was observed in the clad region. In the bonding zone, a few ZrO_2 particles with resolidified Ni-based solid solution and $(Fe,Cr)_{23}C_6$ carbide coexist. An irregular solidified interface between the ceramic layer and the bonding zone offers an excellent fusion bonding. The fine white ZrO_2 particles resolidifying in the bonding zone locally segregate at the boundaries of γ-Ni grains in the form of a flower-like morphology. This can be verified by the compositional image of elemental Zr shown in Fig. 2(b). Table 1 gives the results of energy-dispersive X-ray analysis at the locations indicated in Fig. 2(a). A high content of elemental Fe within the γ-Ni solid solution was produced by oversufficient laser energy.

The compositional line analyses of the elements Zr, Y and Ni and the morphology of white particles with a high content of Zr in the bonding zone (labelled BZ) are shown in Fig. 3. The small black areas are considered as the $(Fe,Cr)_{23}C_6$ carbide deeply etched by 1 mol% NaOH electrolyte. It can be seen that in the ceramic layer a large number of Zr and Y atoms and few Ni

Table 1
Composition (weight per cent) of the indicated locations in the bonding zone

Measurement location	Zr	Ni	Cr	Fe	Si	Y
A	96.8	0.2	0	0	0	3
B	0	48.5	3.9	42.77	4.83	0
C	96.5	0	0	0	0	3.5

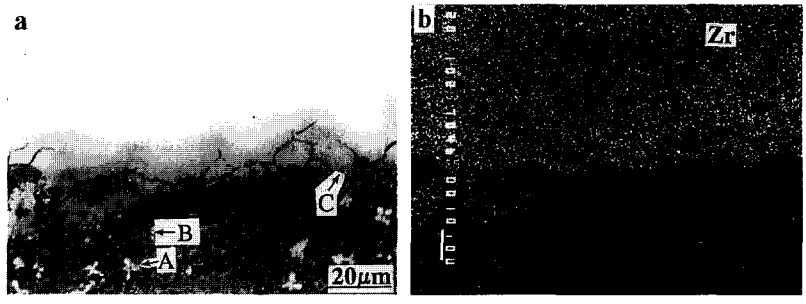

Fig. 2. Bonding characteristic between the ceramic layer and the bonding zone: (a) morphology; (b) Zr distribution in the same area as (a).

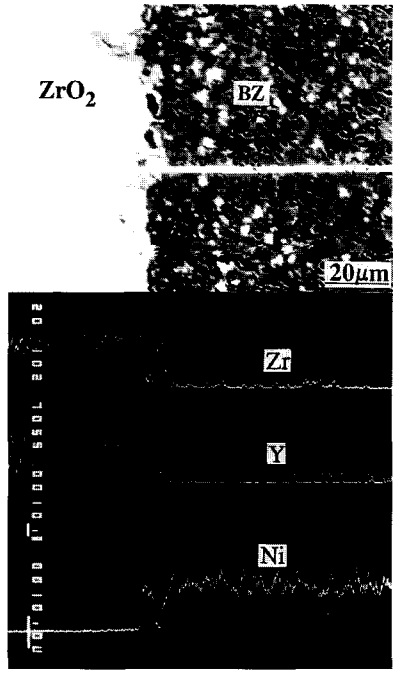

Fig. 3. Compositional line analyses for laser-clad ZrO_2–(Ni alloy) composite coating.

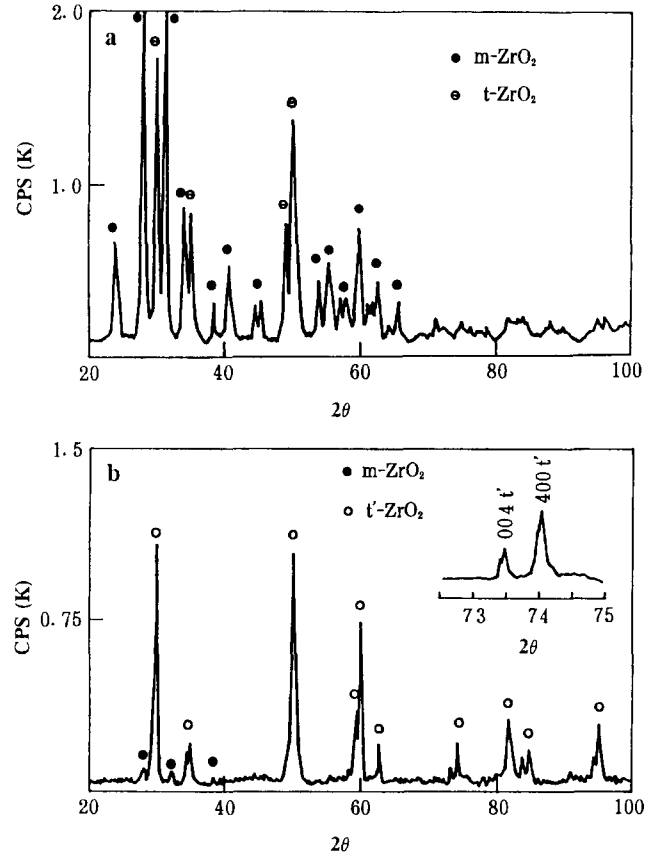

Fig. 4. X-ray diffraction patterns of (a) original ZrO_2 powder and (b) laser-clad ZrO_2 ceramic layer.

atoms were examined. However, in the bonding zone a high content of Ni exists. Such a phenomenon of layering confirms that the elemental Ni has a strong affinity with the steel substrate under the condition of convection in the laser-molten pool. This result will offer a new basis for producing ceramic coatings with an absence of porosity and microcracks. The Ni alloy with a low melting point can be considered as a binder and it can eliminate the stresses and avoid the formation of microcracks on solidification of the ZrO_2 ceramic coating.

The X-ray diffraction patterns of original ZrO_2 powder and laser-clad ZrO_2 ceramic layer are shown in Fig. 4. The original ZrO_2 powder consists of 34 wt.% t-ZrO_2 and 66 wt.% m-ZrO_2 phases, but the clad ZrO_2 ceramic layer consists of 91.4 wt.% t'-ZrO_2 and a very small amount of m-ZrO_2 phases. This can be interpreted by the rapid heating and cooling process of laser cladding. The high cooling rate (about 10^5 °C s^{-1}) restrains the t→m phase transformation in ZrO_2 ceramics and more t'-ZrO_2 phase is produced by diffusionless transformation from the high temperature c phase of ZrO_2. The previous investigations [10–12] indicated that the t' phase does not transform on annealing at 1200 °C for a long time, which is of importance in relation to the service behaviour of a thermal barrier coating.

Fig. 5 shows the morphology of ZrO_2 grains resolidifying in the ceramic layer. The clad ceramic layer exhibits fine equiaxed ZrO_2 grains in the upper part and columnar ZrO_2 dendrites in the lower part growing from the ceramic layer–bonding zone interface. This kind of resolidifying morphology of ZrO_2 grains is in close relationship with the cooling rates in different zones of the ceramic layer. The high temperature caused by laser cladding leads to the melting of ZrO_2 powders, which resolidify and almost completely transform to the metastable tetragonal phase (t') with a twinned morphology as shown in Fig. 5. Only 8.6 wt.% m-ZrO_2 phase was obtained in the ceramic layer on rapid solidification and it is distributed along the boundaries of t'-ZrO_2 grains.

3.2. Microhardness distribution

The distribution of microhardness in laser-clad ZrO_2–(Ni alloy) composite coating is shown in Fig. 6. Three distinct steps can be found in the curves corresponding to the ceramic layer, bonding zone and substrate. Under the processing parameters of 1000 W laser power and 8 mm s^{-1} scanning speed of the laser beam, the average value of microhardness of ZrO_2 ceramic layer is about 1700 $HV_{0.2}$, which is also a maximum with the change in processing parameters. After the laser power is decreased to 800 W, the microhardness and thickness of ceramic layer decrease correspondingly to 1450 $HV_{0.2}$ and 0.1 mm respectively.

Fig. 7 shows the relationship between the average value of microhardness of the ceramic layer and the

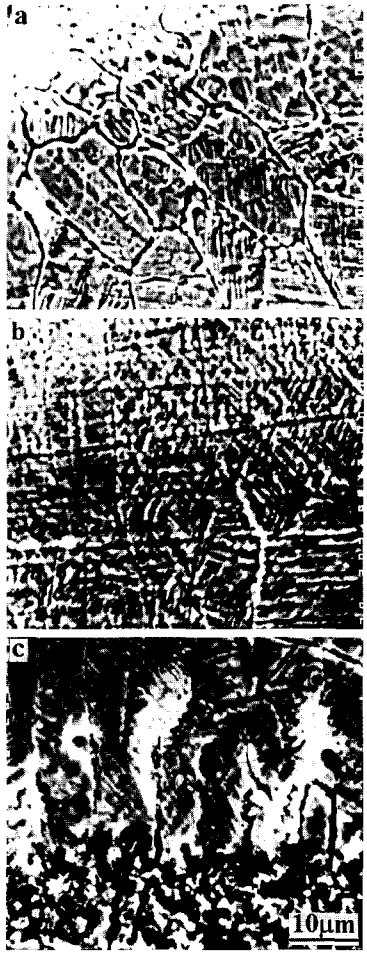

Fig. 5. Morphology of ZrO_2 grains in the ceramic layer (etched by boiled HF acid): (a) at outer part; (b) at intermediate part; (c) at inner part.

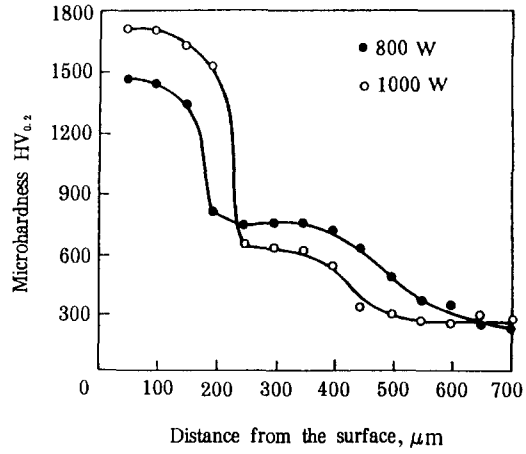

Fig. 6. Distribution of microhardness in laser-clad ZrO_2–(Ni alloy) composite coating ($V = 8$ mm s^{-1}, $D = 3$ mm).

scanning speed of the laser beam at constant laser power and beam diameter. The microhardness of the ceramic layer exhibits a maximum at a certain scanning speed (8 mm s^{-1} for $P = 800$ W and 10 mm s^{-1} for $P = 1000$ W) owing to the effect of cooling rate on the resolidifying microstructure of ZrO_2 grains. Too slow a scanning speed coarsens the ZrO_2 grains, while very high scanning speed leads to molten droplets or poor surface quality of the coating.

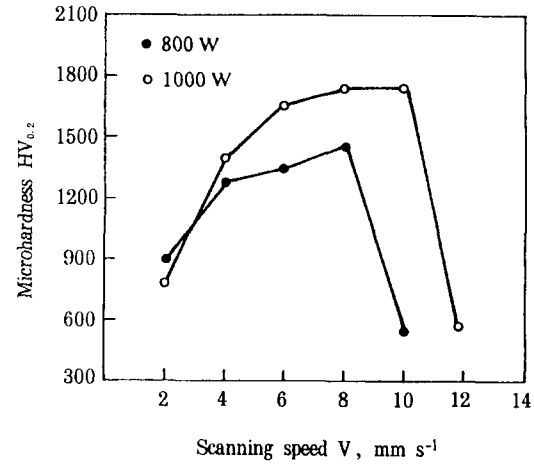

Fig. 7. Effect of the scanning speed of the laser beam on the average value of microhardness of the ceramic layer.

4. Summary

Based on the analysis of the microstructure and microhardness of laser-clad ZrO_2–(Ni alloy) composite coating, a good fusion bonding with an absence of porosity and microcracks between ceramic layer and substrate can be obtained under the processing conditions of 1000 W laser power, 10 mm s^{-1} scanning speed of the laser beam and 3 mm beam diameter. The rapid cooling rate restrains the formation of m-ZrO_2 phase and benefits the production of metastable tetragonal phase t'-ZrO_2 during resolidification. Such a pure ZrO_2 ceramic layer with a high thermal stability of the t' phase may offer excellent thermal and chemical properties in high temperature applications.

References

[1] K.M. Jasim, R.D. Rawlings and D.R.F. West, *Surf. Coat. Technol., 53* (1992) 75–86.
[2] G. Gravanis, A. Tsetsekou et al., *Surf. Coat. Technol., 45* (1991) 245–253.
[3] P.Yu. Pekshev and I.G. Murzin, *Surf. Coat. Technol., 56* (1993) 199–208.
[4] A. Petitbon and D. Guignot, *Mater. Sci. Eng., A121* (1989) 545–548.
[5] H.L. Tsai, P.C. Tsai and D.C. Tu, *Mater. Sci. Eng., A161* (1993) 145–155.

[6] P.C. Tsai, H.L. Tsai and D.C. Tu, *Mater. Sci. Eng., A165* (1993) 167–173.
[7] A. Wang, B. Zhu, Z. Tao, X. Ma, S. Deng and X. Cheng, *Surf. Coat. Technol., 57* (1993) 169–172.
[8] K.M. Jasim, R.D. Rawlings and D.R.F. West, *J. Mater. Sci., 27* (1992) 3903–3910.
[9] I. Smurov, A. Uglov, et al., *J. Mater. Sci., 27* (1992) 4523–4530.
[10] B.C. Wu, E. Chang, S.F. Chang and D. Tu, *J. Am. Ceram. Soc., 72* (1989) 212–218.
[11] A. Bennett, *Mater. Sci. Technol., 2* (1986) 257–261.
[12] K.M. Jasim, R.D. Rawlings and D.R.F. West, *Mater. Sci. Technol., 8* (1992) 83–91.